Lawrence Livermore National Laboratory

LLNL-JRNL-2015314

Comparison of URANS and LES predictions for the open phase of the OECD NEA CSNI fluid structure interaction CFD benchmark

J Solberg

February 2026

Nuclear Engineering and Design

This work performed under the auspices of the U.S. Department of Energy by Lawrence Livermore National Laboratory under Contract DE-AC52-07NA27344.

Highlights

Comparison of URANS and LES Predictions for the Open Phase of the OECD NEA CSNI Fluid Structure Interaction CFD Benchmark

Graham Macpherson, David Munn, Alan Johnson, Landon Brockmeyer, Elia Merzari, Jerome Solberg

- Contributions to an international benchmark for fluid–structure interaction (FSI) simulation.
- CFD predictions that are in good agreement with many aspects of experimental FSI data.
- Clear conclusions and guidance on the limitations of URANS for FSI predictions.

Comparison of URANS and LES Predictions for the Open Phase of the OECD NEA CSNI Fluid Structure Interaction CFD Benchmark

Graham Macpherson[a,*], David Munn[a], Alan Johnson[a], Landon Brockmeyer[b], Elia Merzari[c], Jerome Solberg[d]

[a] *Frazer-Nash Consultancy, United Kingdom*
[b] *Argonne National Laboratory, USA*
[c] *The Pennsylvania State University, USA*
[d] *Lawrence Livermore National Laboratory, USA*

Abstract

The OECD NEA CSNI WGAMA CFD Task Group ran a benchmark in 2020 and 2021 to assess the predictive capabilities of coupled fluid structure interaction (FSI) CFD analysis methods. This paper presents the predictions made for the open phase of the benchmark using URANS and LES turbulence modelling approaches, and a comparison of the results to the experimental data.

The benchmark comprised a channel containing two inline cylinders in cross-flow. The cylinders were fixed at one end, free at the other, and had measured resonant frequencies and damping properties. The URANS modelling used ANSYS Fluent 2-way coupled to ANSYS Mechanical. The LES modelling used Nek5000, 1-way coupled to Diablo. Comparisons with cross-channel velocity profiles are presented, both for the mean flow and its RMS. Comparisons are also made to the frequency spectra for point measurements of fluid velocity and pressure, and for the accelerations of the free end of each cylinder.

URANS predicts the average velocity profiles relatively well, and is able to predict the velocity and acceleration spectra at the shedding frequency. However, the frequency content at the 4th harmonic of the shedding frequency is low in the URANS flow fields, and so does not excite accelerations

*g.macpherson@fnc.co.uk

Preprint submitted to Nuclear Engineering and Design *January 5, 2026*

at the resonant frequency of the cylinders. LES makes better predictions of the average profiles, and the velocity spectra agree well at both the shedding frequency and at higher frequencies. The 1-way coupled LES results show good agreement for acceleration spectra.

Keywords:
CFD, FSI, URANS, LES, Validation, Coupling

---

1. Introduction

OECD NEA CSNI WGAMA[1] CFD Task Group considers the application of Computational Fluid Dynamics (CFD) for nuclear reactor safety related assessments. It publishes best practice guidelines, organises the Computational Fluid Dynamics for Nuclear Reactor Safety (CFD4NRS) workshop series, and conducts international benchmarking activities. Their recent Technical Opinion Paper (CSNI, 2024b) provides more context.

In 2020 and 2021 the CFD Task Group ran a benchmarking study to assess the predictive Fluid Structure Interaction (FSI) capabilities of CFD coupled to Computational Structural Dynamics (CSD). The benchmark comprised a channel containing two inline cylinders in cross-flow. The cylinders were fixed at one end, free at the other, and had measured resonant frequencies and damping properties. The benchmark had an 'open' phase, where the experimental setup, boundary conditions and experimental results were available to the participants, and a 'closed' phase, where only the setup and boundary conditions were provided, and predictions were submitted 'blind', for comparison. The benchmark specification (CSNI, 2024a) is now publicly available, and details of the open phase have been previously published (Bolshukhin et al., 2021). The results of the closed phase are available from the official benchmark report (CSNI, 2024a).

1.1. Experimental Data

The experimental data (CSNI, 2024a; Bolshukhin et al., 2021) comprises several types of information, whose measurement locations are shown in Figure 1:

[1]The OECD Nuclear Energy Agency's Committee for the Safety of Nuclear Installations, Working Group on the Analysis and Management of Accidents.

- Averaged profiles of mean and RMS streamwise and transverse velocity on four lines across the flow domain, at locations in the wake of the cylinders (v_1, v_2, v_3, v_4). These profiles were taken on planes at three heights (h_1, h_2, h_3), giving 12 lines.
- Streamwise velocity time series at point locations on the same profile lines (v_1, v_2, v_3, v_4), offset from the cylinder centrelines. The velocity measurements are made by PIV and LDV.
- Pressure time series at four locations on the channel wall (p_1, p_2, p_3, p_4).
- Acceleration time series in the streamwise (a_{1x}, a_{2x}) and transverse (a_{1y}, a_{2y}) directions from accelerometers mounted in the tips of each cylinder.

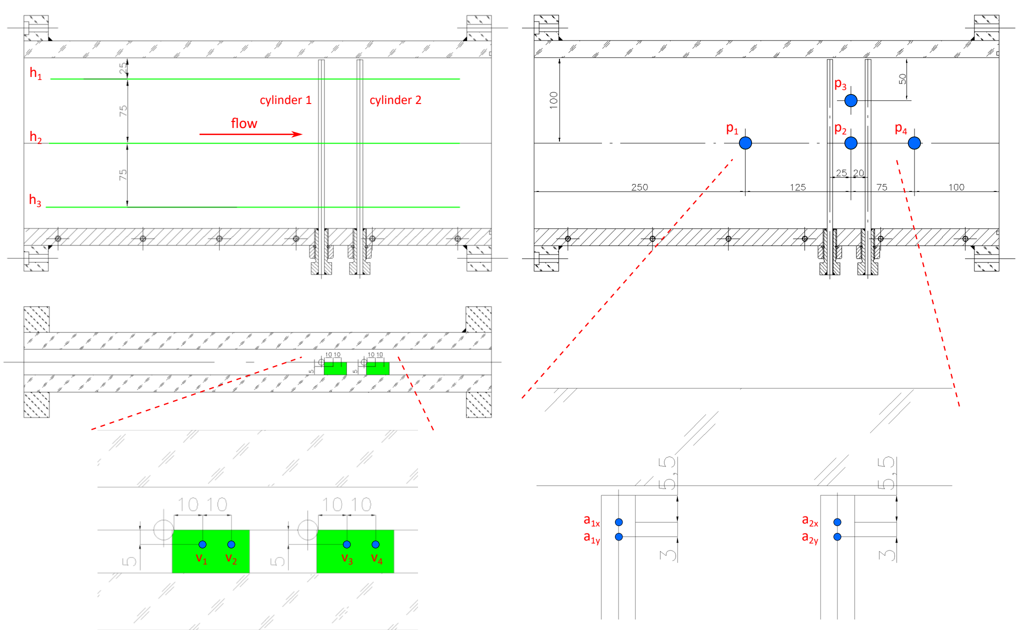

Figure 1: Velocity, pressure and acceleration instrumentation. Adapted from CSNI (2024a).

The time series are sampled at high frequency and provide data of approximately 150 s duration. The averaged velocity profiles are similarly the result of a large number of data samples. This highlights a particular challenge in transient CFD analysis compared to experimental assessments; computational costs are high, run times are long, and so the simulated duration will be short, leading to noisier and less well resolved data for comparison. Profiles of mean and RMS velocities upstream of the cylinder on a vertical centreline and four equally spaced horizontal lines were provided, allowing 2D profiles of velocity and turbulence to be created as a realistic inlet condition. Data and boundary conditions for two flow conditions were provided in the open phase of the benchmark:

Low flow: $10\,\mathrm{m}^3/\mathrm{hr}$.

High flow: $16\,\mathrm{m}^3/\mathrm{hr}$. In this case, the cylinder motion experienced 'lock-in' where the motion of the cylinder and the vortex shedding in the flow became synchronised, substantially amplifying the motion.

The two cylinders were 7 mm diameter, 198 mm long and separated in the streamwise direction by 45 mm in a 30 mm wide, 200 mm high channel. The mass distribution and material properties of the cylinders were provided, as well as their dynamic properties measured from impact excitation tests, providing data for natural frequencies and damping. In the work reported here, it was assumed that the rest of the channel, especially its base plate, were sufficiently stiff that their dynamics were not important, and that the CSD models would comprise two unconnected cylinders that were fully fixed at their base. The natural frequencies were 98 Hz for the first cylinder and 90 Hz for the second (in water); the difference between them was intentional.

2. CFD and CSD Methods

The work described was carried out by two groups in close collaboration. The intention was to assess how good the predictions of a Large Eddy Simulation (LES) CFD solution could be compared to the experimental data, but also what was able to be captured by an Unsteady Reynolds-Averaged Navier-Stokes (URANS) approach (noting its reduced computational expense but reduced resolution of turbulence).

The URANS methodology was informed by ANSYS's training and guidance materials:

Structural, ANSYS Mechanical APDL 20.1: 2600 quadratic shell elements for cylinders with midside nodes – localised density changes for

mass distribution.
Frequency dependent damping using alpha and beta terms (Ansys, 2020, Rayleigh Damping) determined at 90 Hz and 90/4 Hz.

Fluid, ANSYS Fluent 20.1: k-ω SST URANS. IAPWS water properties at 10°C, using compressible liquid formulation.
7 million cells – vertically swept quad-dominated profile with $y^+ \approx 1$ (Figure 2). Diffusion based smoothing of cylinder displacement for dynamic mesh.

Coupling, ANSYS System Coupling: 2-way iteratively coupled – forces sent from fluid to structural, displacements returned from structural to fluid. 4 coupling iterations per timestep.
1-way coupled acoustic model also implemented.

Solution: Timestep of 5×10^{-4} s for 10 m^3/hr, 3.125×10^{-4} s for 16 m^3/hr, 4 fluid iterations per coupling iteration. Startup used a linear velocity ramp for 1 s from 10% to full flow, then 1 s transient wash-through was discarded and data gathered for 6 s (10 m^3/hr) or 3.75 s (16 m^3/hr) – 12000 timesteps. The solution required approximately 1 week on 256 cores (2 used for CSD).

The LES methodology had been previously applied to relevant FSI problems (Brockmeyer et al., 2019, 2020):

Structural, Diablo, customised version for FSI: FEA solver developed at Lawrence Livermore National Laboratory. 3D solid elements (20,068 nodes and 13,824 8-node hexahedral elements). Linear elasticity and standard B-Bar formulation. Mass tuned to match to the natural frequency in water, mass and stiffness damping matched to data – frequencies chosen for Rayleigh damping at the first cylinder natural frequency and a quarter of it.

Fluid, Nek5000 v19: Spectral element open source fluid solver. Incompressible formulation LES with explicit filtering. 114,576 hexahedral elements, polynomial order N = 7 (40 million grid points).

Coupling: Coupled via basis-function interpolation of the surface pressure only. 1-way coupled results only; 2-way coupled solutions were not realised in the benchmark time frame.

Solution, fluid only: Timestep of 1.5×10^{-4} s for $10\,\mathrm{m^3/hr}$, 1.275×10^{-4} s for $16\,\mathrm{m^3/hr}$. Data gathered for 1.824 s ($10\,\mathrm{m^3/hr}$) or 1.390 s ($16\,\mathrm{m^3/hr}$).

Solution, 1-way coupled: Fluid timestep of 5×10^{-5} s, structural timestep of 5×10^{-6} s. Gradual ramp of forces applied to structure from developed flow solution. 0.488 s data gathering solution for $10\,\mathrm{m^3/hr}$ only.

The adequacy of each mesh was assessed using engineering judgement and inspection of the solution. The meshes were designed for high cell quality, and adhered to good practice for first cell height and expansion ratio for boundary layer resolving solutions. The y^+ values and smoothness of the wall shear-stress provided confidence in the wall-normal and circumferential resolution and the smoothness of the velocity and turbulence fields in the bulk of the fluid domain was also assessed.

The effect of polynomial order (hence resolution) in the Nek5000 solution on the frequency spectrum for forces transferred to Diablo was evaluated and used to establish the appropriate choice. This also determined the time step and therefore the overall the computational cost.

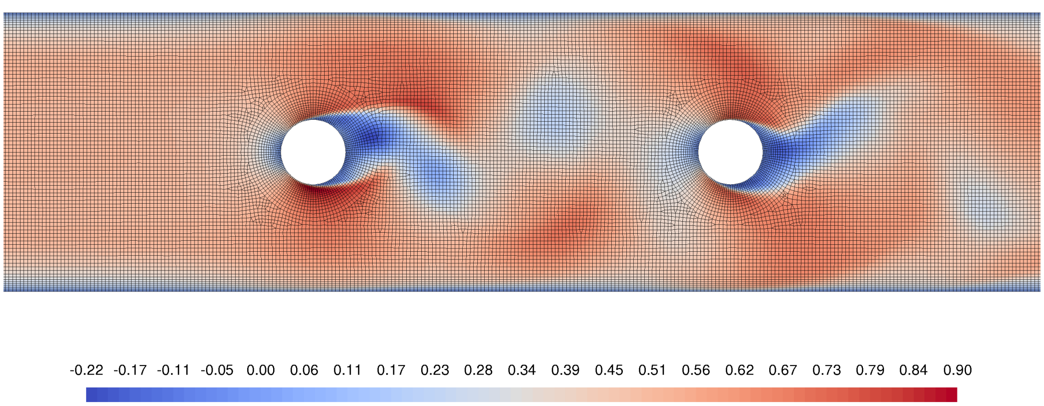

Figure 2: URANS mesh at mid-height plane showing a snapshot of streamwise (channel flow direction) velocity for the low flow case. Thick boundary layer mesh on cylinders allows mesh motion to be accommodated, maintaining cell and solution quality.

3. Results

The geometry, material properties of the water and flow rates were combined to assess the Reynolds number and estimate the expected vortex shedding frequencies. These values are shown in Table 1, and have variants that account for the blockage effect of the cylinder (7 mm/30 mm = 23.3%), which causes an increase in the apparent free-stream velocity as the flow passes it. More emphasis is placed on the low flow (10 m^3/hr) flow results below, because the comparison is easier and clearer, since there is no lock-in present in the data.

Table 1: Flow characteristics and expected frequencies.

Flow (m^3/hr)	10	16
Mean U (m/s)	0.463	0.741
Flow time between cylinders (s)	0.097	0.061
Re Channel	10632	17012
Re Cylinder	2481	3969
Mean U with blockage (m/s)	0.604	0.966
Re Cylinder with blockage	3236	5177
Strouhal number (Blevins, 2001)	0.197	0.197
f shedding (Hz)	13.0	20.9
f shedding with blockage (Hz)	17.0	27.2

3.1. Low Flow Results

Figure 3 shows the displacement at the accelerometer locations for the URANS case. The streamwise displacement does not have a zero mean, since the drag on the cylinder produces a constant deflection. The mean streamwise deflection of the upstream cylinder, a_{1x}, is greater, and the variation in the downstream deflection, a_{2x}, is much greater. The startup process can be seen in the discarded time before 0 s, where the initial perturbation to start the flow at 10% makes the cylinder 'ring' in the streamwise direction for approximately 0.1 s, and it takes until about 0.5 s for vortex shedding to begin, and produce transverse displacements. The transverse displacements of the downstream cylinder, a_{2z}, are substantially greater than the upstream displacements.[2] The streamwise and transverse displacements both exhibit intermittent periods of high and low motion. This intermittency is present in the experimental data, and could be worthy of further study in itself, especially since it is produced by the URANS modelling (i.e. does not rely on resolved turbulence).

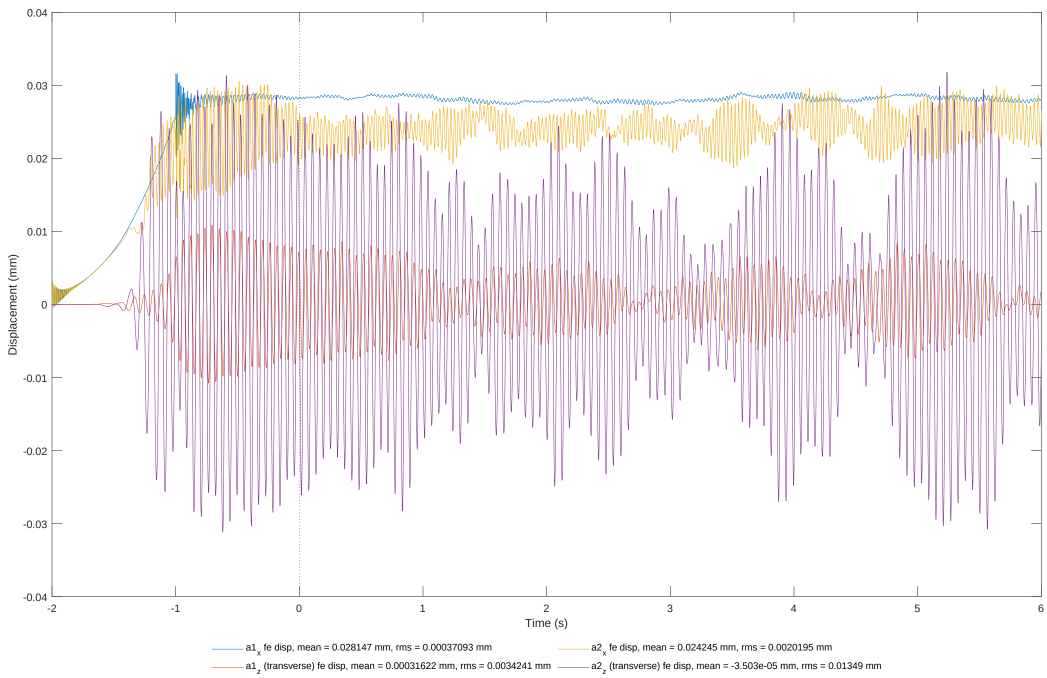

Figure 3: Cylinder displacements at accelerometer locations for 2-way coupled URANS for the low flow case.

Figures 4 and 5 show field plots illustrating the flow features seen, and also indicate the line and point measurement locations for the velocity profiles and velocity spectra. Figure 5 shows that a jet passes through the 2 mm gap between the cylinder tip and descends into the cylinder wake. It also shows the complex pattern of vortex shedding that is not coherent with cylinder height.

The averaged profiles of mean and RMS streamwise velocities are shown

[2]There is a coordinate system inconsistency between the URANS and the LES and experimental data; the x direction is always streamwise, but y and z are both used for transverse; the figure legends clarify where needed.

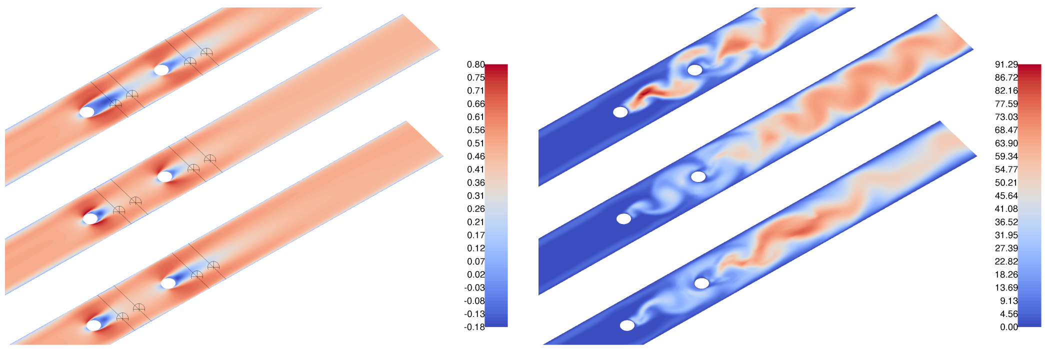

Figure 4: Flow on the three velocity measurement planes (h_1 to h_3, Figure 1) for the low flow case. Left: averaged URANS streamwise velocity (m/s), showing profile lines and spectrum sampling locations (v_1 to v_4) per plane. Right: snapshot of turbulent viscosity ratio showing vortex shedding structures.

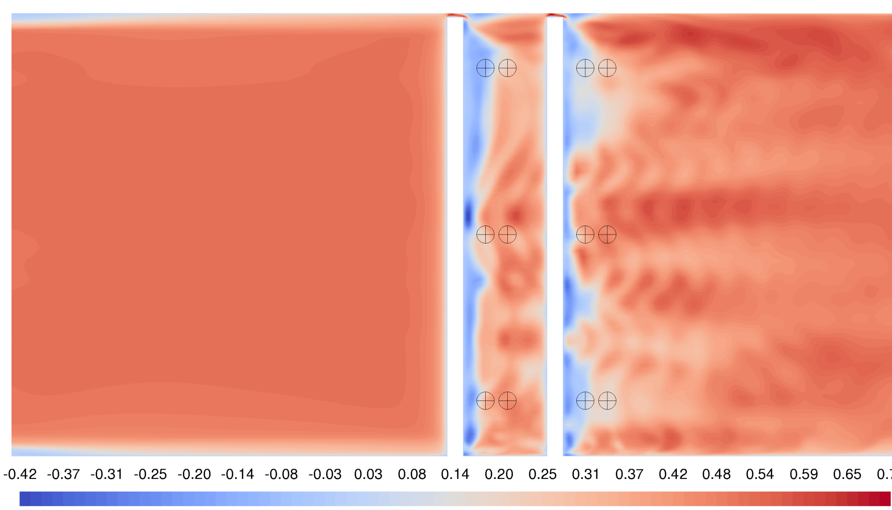

Figure 5: Snapshot of URANS streamwise velocity (m/s) through the cylinder midplane for the low flow case. Velocity spectrum sampling locations v_1 to v_4 are shown at each height, h_1 to h_3.

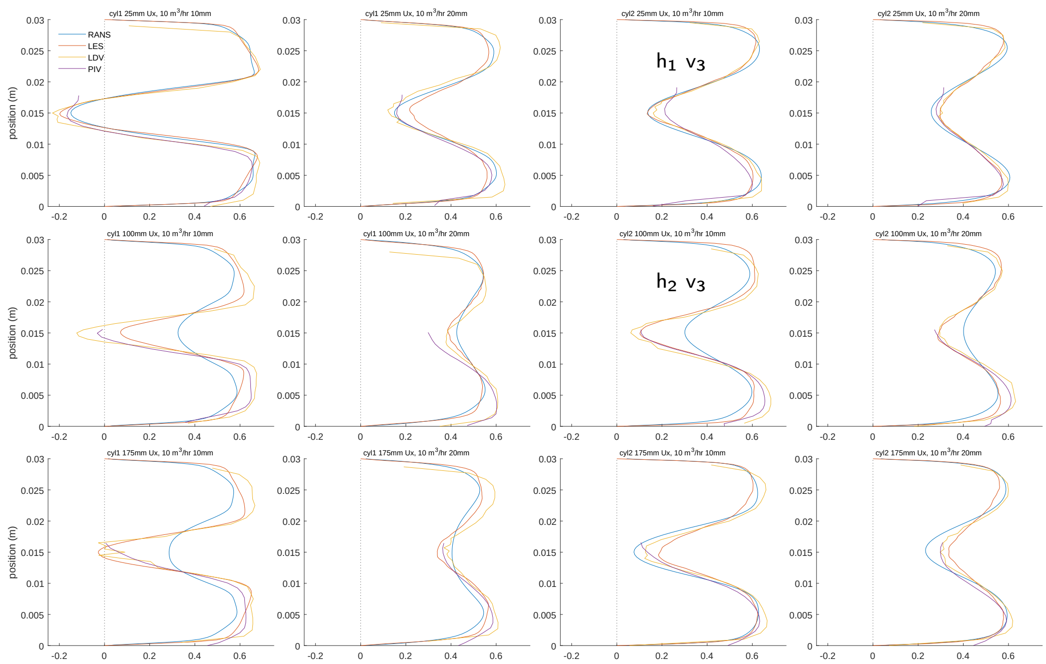

Figure 6: Mean streamwise velocity profiles comparing URANS, LES and experimental (LDV, PIV) data for the low flow case. The top row is v_1 to v_4 on h_1 (top of the channel) from left to right, the mid row is h_2 and the bottom row is h_3. The velocity spectra for the two locations noted (v_3 at h_1 and h_2) are shown on Figure 8 and 9.

in Figures 6 and 7. In general, the agreement of the LES with the experiment (with the LDV data especially) is good. The profile shapes and values are in good agreement, including, for example, the peaks in RMS near to the channel walls.

The URANS agreement is more mixed; in some places, it is excellent, but in others, it deviates significantly. For mean flows, however, small positional differences in the profile sampling line would give very different results, i.e. at v_1 for h_2 and h_3, the URANS agreement is not good, but if either the sampling line were moved slightly upstream, or the mean extent of separation/wake were slightly larger, then the figure would change significantly. For the RMS results, the URANS results are lower, as expected, given the lack of resolved unsteadiness. In some locations the shape (if not magnitude) is in agreement, but in others, it is different, and it does not represent the 'wall peaks' well.

Figure 8 shows example time domain data, which illustrates that the URANS variation is qualitatively different compared to the LES and experimental data. This is seen in the frequency spectra on the same figure, where the URANS representation of the peak at the shedding frequency is good, but at higher frequency, the content reduces sharply, compared to the LES result, which follows the experimental data well. This is a good illustration of what URANS is expected to do; it has filtered almost all higher frequency content, and included it in the eddy viscosity, but still resolved the largest unsteady vortex structures. Welch's method was used to average overlapping time windows to estimate the spectra; the choice of settings is a trade-off between better resolution and more averaging to reduce noise. Information about the window lengths and frequency resolution is given in the title above each figure. The velocity spectra for the experimental data and both CFD predictions show slightly lower shedding frequencies at the top and bottom compared to the middle (not shown in figures), caused by the presence of the wall, and the shedding frequency agrees well with the estimate 'with blockage' from Table 1.

Spectra corresponding to two velocity profile locations from Figure 6 are shown in Figure 8 and 9. For h_1 v_3 the URANS profile and spectra agreement with the experiment is good. For h_2 v_3 the URANS profile agreement is worse, the double peak around the shedding frequency is not captured, and the shape of the RMS profile is not correct in Figure 7. The agreement of the LES result is good in both locations. Figure 9 also shows a pressure spectrum, similarly showing that, around the shedding frequency, the URANS and LES results agree with the experiment, but at higher frequency, the URANS solution contains less content, and more distinct 'harmonics'.

The averaged profiles of mean and RMS transverse velocities are shown in Figures 10 and 11. Similar conclusions as for the streamwise profiles can be drawn. In general, the agreement of the LES with the experimental data is good, but more mixed for URANS. The RMS agreement for URANS is relatively good, where the transverse variability is expected to be dominated by the large shed vortices, which it resolves.

Comparisons of acceleration spectra for the downstream cylinder are shown in Figure 12. As expected, the first fluid peak[3] in the streamwise direction is twice the shedding frequency (this can also be seen in Figure 3). The length of data gathered for the LES solution is insufficient to provide an accurate spectrum at the shedding frequency, however, the agreement near to the cylinder natural frequency (90 Hz) is very good. The natural frequency is approximately four times the shedding frequency, so the cylinder motion is driven by the fourth harmonic of the vortex shedding. This explains why the URANS solution agrees well with the acceleration peaks at the shedding frequency, but not at higher frequency – there is a lack of excitation in that range. Comparing 1-way and 2-way coupled URANS solutions (not shown in figures) showed similar acceleration responses, with only modest differences at higher frequencies, and little difference around the shedding frequency.

3.2. High Flow Results

The high flow ($16\,\mathrm{m}^3/\mathrm{hr}$) URANS case was solved in the same way as the low flow case. It produced comparable results, but should not have. In the experimental data, the velocity spectra show that the shedding frequencies are the same at each height, showing the synchronising effect of lock-in. This is not seen in the CFD results. No LES solutions are presented here, because 1-way coupling has no ability to represent lock-in.

The acceleration spectra shown on the left of Figure 13 indicates the problem. Although the lowest URANS peak at around 50 Hz matches the data, there is a substantial disagreement at around 90 Hz, where the experimental accelerations are orders of magnitude higher. Comparing the ratio of the peaks for URANS accelerations from the two flows on the right of the same figure shows that there is some elevated response at higher frequency in the

[3] The frequency content in the experimental data below 10 Hz is interpreted as experimental equipment vibration.

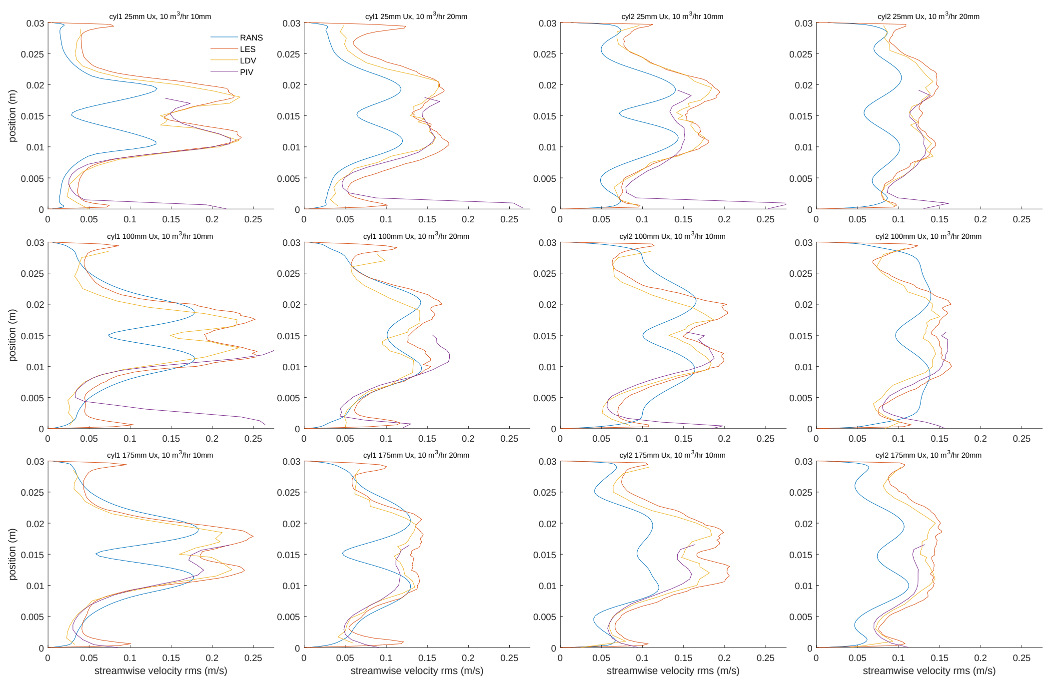

Figure 7: RMS streamwise velocity profiles comparing URANS, LES and experimental (LDV, PIV) data for the low flow case. Layout equivalent to Figure 6.

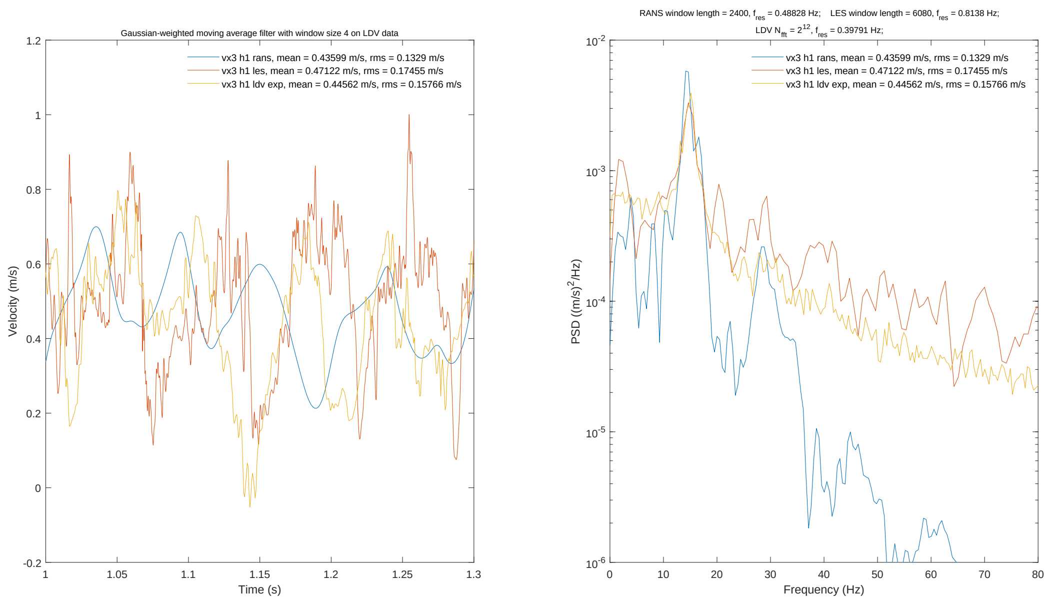

Figure 8: Example of time domain (left) and frequency spectra (right) for location h_1 v_3, comparing URANS, LES and experimental data for the low flow case.

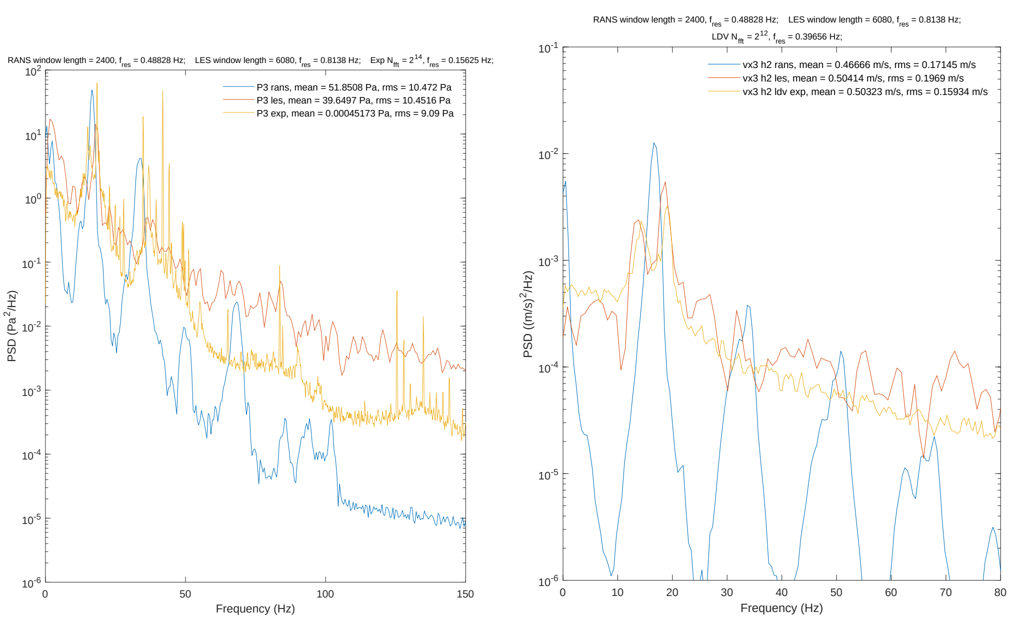

Figure 9: Further comparisons of URANS, LES and experimental data for the low flow case. Left: Pressure spectra at p_3. Right: Velocity spectra at h_2 v_3 (mid-height, as per Figure 6).

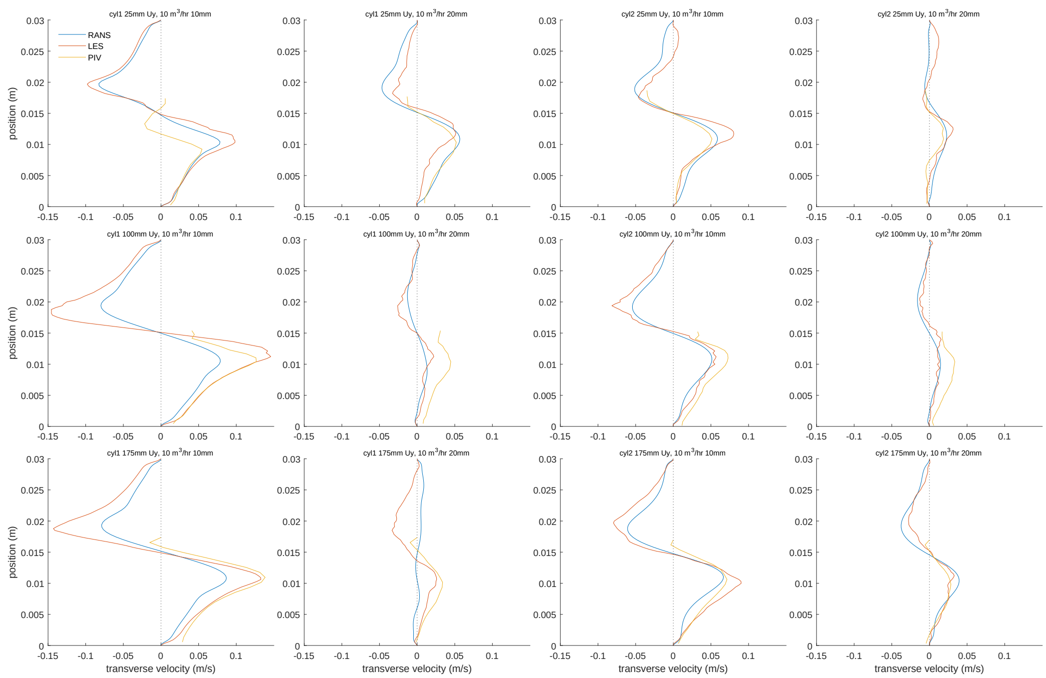

Figure 10: Mean transverse velocity profiles comparing URANS, LES and experimental (PIV) data for the low flow case. Layout equivalent to Figure 6.

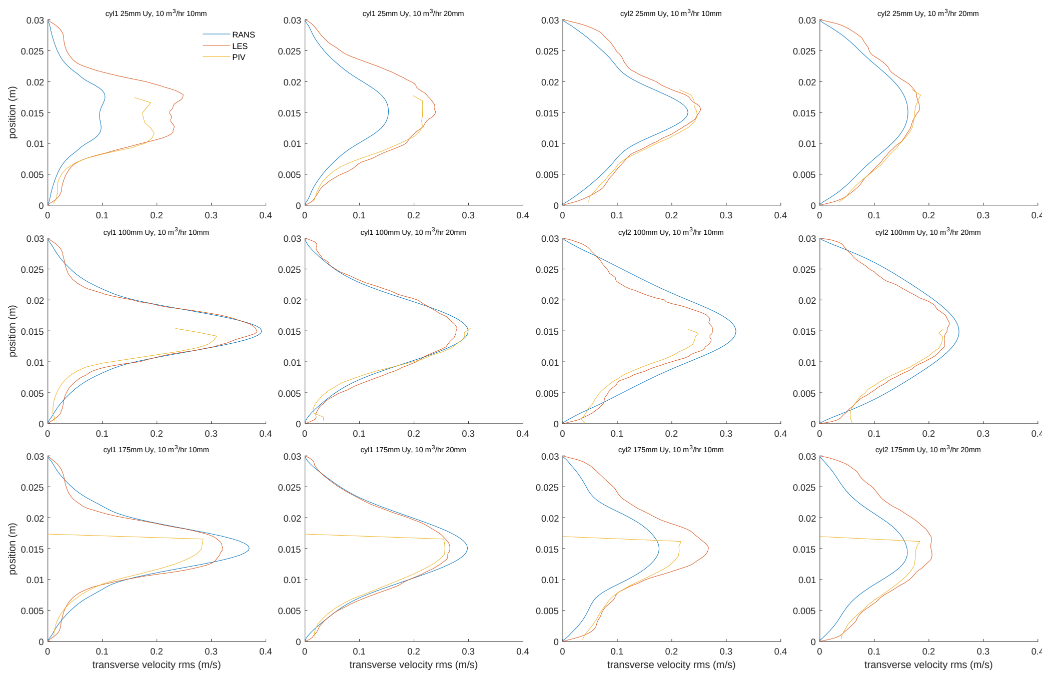

Figure 11: RMS transverse velocity profiles comparing URANS, LES and experimental (PIV) data for the low flow case. Layout equivalent to Figure 6.

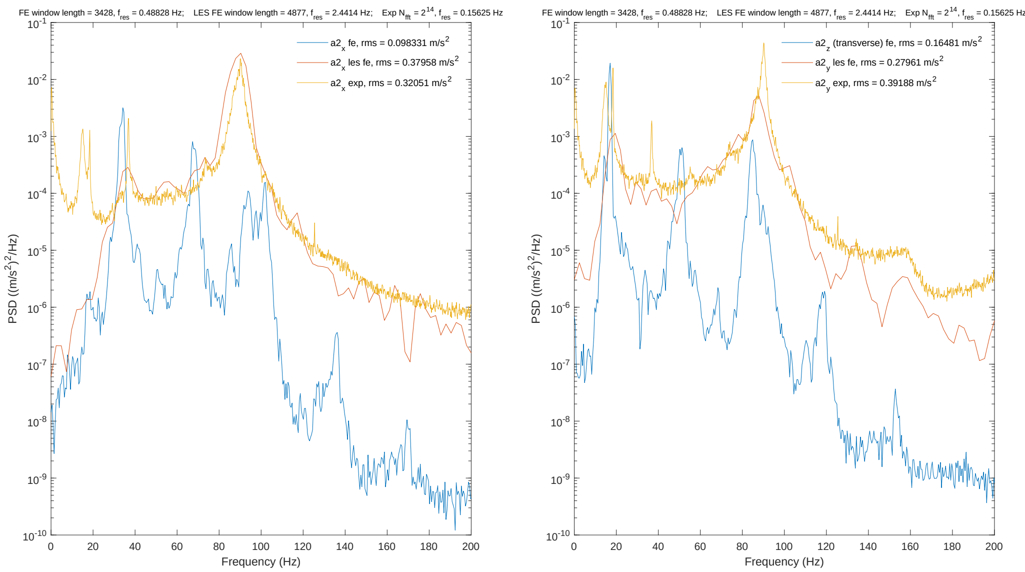

Figure 12: Comparing URANS, LES and experimental data for streamwise (left) and transverse (right) acceleration of cylinder 2 (downstream, locations as per Figure 1) for the low flow case. In the legend 'fe' refers to the URANS predictions, whereas 'les fe' refers the LES predictions.

high flow case. This shows that there is some amplification at the natural frequency, but not enough excitation to cause sufficiently large motions that affect the flow, resonate and cause lock-in.

4. Conclusions

The benchmark results show that URANS is able to predict average profiles with moderate accuracy, and to predict the velocity and acceleration spectra reasonably well at shedding frequencies for both flow speeds. However, the nature of this experiment means that the lack of fourth harmonic frequency content in the URANS solution means that it does not excite that cylinder in the regions of the natural frequencies (90 to 100 Hz). Therefore, lock-in was not able to be predicted by URANS for the 16 m^3/hr case, even with 2-way coupling and a dynamic mesh. LES was shown to predict mean and RMS velocity profiles well, the velocity spectra agree well at shedding frequency, and also have correct higher-frequency behaviour. 1-way coupled 10 m^3/hr LES results show good agreement for acceleration spectra, especially around cylinder 2's natural frequency.

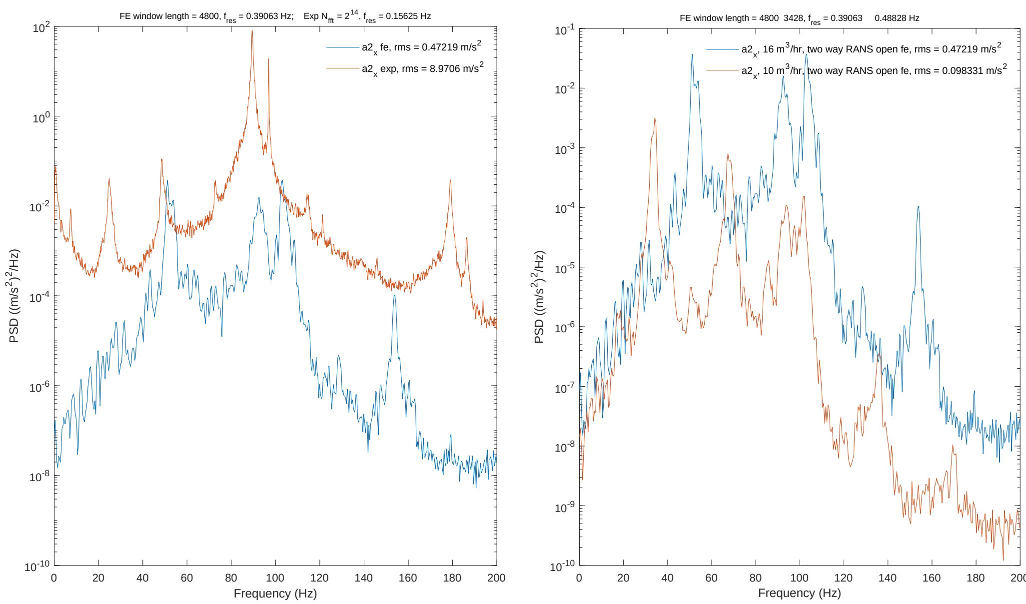

Figure 13: Left: URANS cylinder 2 streamwise acceleration predictions compared to high flow experiment. Right: comparison of URANS cylinder 2 streamwise accelerations between the two flows.

Given the good predictions at the natural frequencies, it is likely that 2-way coupled LES would be able to simulate lock-in conditions, but given the short timesteps required, and the unknown timeframe needed for the flow and motion to synchronise and resonant condition to develop, it is very computationally expensive. We could not achieve this during this collaboration for this benchmark, but note that ongoing work using GPU acceleration for the fluid solution shows good promise (Bistany et al., 2024). It is also likely that URANS also could predict lock-in, but only if the structural excitation was from the fundamental shedding frequency. Whether this is true will be difficult to assess in advance, or will vary for more complex flows and geometries. This also leads to a question around how truly predictive of specific geometries and flows these methods can be. If predicting the response relies on experimentally well-characterised structural models of the specific geometry (as this benchmark case did), then the utility of CFD studies will be more applicable to generic situations.

This benchmark is also a good example of why rigorous sensitivity analysis and uncertainty quantification is hard for more complex simulations (Macpherson and Headings, 2022). To perform sensitivity and uncertainty studies for the choice of RANS model, numerical settings, mesh resolution, timestep etc would mean comparing to averaged profile and spectral data for a range of physical quantities, each of which have a number of features that could be quantitatively assessed. Each simulation would need to be run for sufficiently long (which is computationally expensive) such that the averaged profiles and spectra converged sufficiently to allow the differences in the results caused by changes in configuration to be visible.

Acknowledgments

This work was made possible by the Nuclear Innovation Programme, funded by the UK Government Department for Business, Energy and Industrial Strategy (now Department for Energy Security and Net Zero).

References

Ansys, 2020. Mechanical APDL Structural Analysis Guide. Technical Report Release 2020 R1.

Bistany, S., Reger, D., Merzari, E., Solberg, J., 2024. Toward a GPU accelerated framework for high-fidelity simulations of flow induced vibrations in nuclear reactors, in: FIV2024.

Blevins, R.D., 2001. Flow-Induced Vibration. Second ed., Krieger.

Bolshukhin, M., Budnikov, A., Shmelev, E., Kulikov, D., Loginov, A., Pribaturin, N., Lobanov, P., Meledin, V., Suvorov, A., Stulenkov, A., 2021. Dynamic measurements of the flow and structure oscillations to validate FSI calculations. Nuclear Engineering and Design 381, 111336. doi:10.1016/j.nucengdes.2021.111336.

Brockmeyer, L., Merzari, E., Solberg, J., Hassan, Y., 2020. One-way coupled simulation of FIV in a 7-pin wire-wrapped fuel pin bundle. Nuclear Engineering and Design 356, 110367. doi:10.1016/j.nucengdes.2019.110367.

Brockmeyer, L., Merzari, E., Solberg, J., Karazis, K., Hassan, Y., 2019. High fidelity simulation and validation of crossflow through a tube bundle and the onset of vibration. International Journal of Non-Linear Mechanics 117, 103231. doi:10.1016/j.ijnonlinmec.2019.07.016.

CSNI, 2024a. The FSI Benchmark Based on OKBM Experiments to Validate Coupled CFD and CSD Calculations. Technical Report NEA/CSNI/R(2023)2. OECD NEA Committee on the Safety of Nuclear Installations.

CSNI, 2024b. Use of Computational Fluid Dynamics for Nuclear Safety. Technical Report CSNI Technical Opinion Paper No. 20. OECD NEA Committee on the Safety of Nuclear Installations.

Macpherson, G., Headings, N., 2022. Why is uncertainty quantification hard for industrial users? Transactions of the American Nuclear Society 126, 340–343.